

# Preliminary Design of Tracking Loop for Marine-Used Machine Gun

Sou-Chen, Lee and Cheng-Yu, Liu

*Chung Cheng Institute of Technology, Taiwan-33 509, Republic of China.*

## ABSTRACT

This study develops conventional use of 20 mm twin machine gun to provide defence against close-in-air threat. For expanding the field of usage of machine gun and promoting defence ability in naval combat, this study offers a preliminary design of tracking loop, which includes the man-in-loop's scheme. Accuracy and stabilisation are the main considerations for a shipboard weapon design and are included in design. In numerical simulations, the stabilisation of gun mount and carriage platform in tracking loop under large disturbances induced by sea waves is assessed first. Two typical scenarios proceed with the testing of tracking performances. Simulation results demonstrate the effective performance of designed tracking loop subject to environmental disturbances.

## 1. INTRODUCTION

A battleship's point defence is the fundamental tactical consideration that provides protection for that single unit. The fire control problem has existed since the early days of World War I. In a naval warfield, the threats mainly come from the air-aircraft and antiship missiles. The ship armed for air defence attempts to shoot down any threat that enters the circle around the ship. Many air defence systems containing missiles and machine guns are developed worldwide. The Marsurca (France), SAN-2, SAN-3 (Russia), Standard 2, Standard 3 (USA), Sea Dart (UK) are well-known area defence missiles with several ten nautical miles fire ranges. For the short range air defence, the Sea Sparrow, Stinger (USA), SA-N-1 (Russia), and Seawolf (UK) are employed to attack the threats several nautical miles away. To treat a

close-in threat, the God Heeper (Holland), Seaguard (Switzerland), Phalanx (USA), Dardo (Italy), Meroka (Spain) and Air Defence Gun (Russia) are the renowned weapon systems that are deployed against a close-in target (within 3 km) with multibarrels.

The renowned T75 20 mm twin machine gun was developed by the Military Combined Service Force (MCSF) Hsin-Ho Machinery Corporation at Kaohsiung, Taiwan, in 1988. The T75 machine gun with open control loop has a high fire rate up to 1500 rounds/min, 1~2 mils accuracy in 2 km, and low cost advantages. It is hoped that the ship equipped with T75 machine gun with redesigned control loop will further strengthen ship's point defence ability.

Accuracy and stabilisation are the primary concerns in designing shipboard weapons. A



to intercept air threats without human determination processes. The Phalanx system is the renowned one.

The T75 twin machine gun was developed to provide a complete defence against low-flying targets at a rather short range<sup>5</sup> (nearly 2 km). Its major characteristics are listed in Table 1. In marine use, its fire control may adapt a direct type that is continuously alert and is controlled by a gunner through an optical aiming device. Figure 1 illustrates the typical driven reticle fire control loop for general weapons<sup>6</sup>. The loop designed here is the simplified one.

Table 1. Characteristics of 20 mm machine gun

	Bearing	Elevation
Moment of inertia*	599.47 kg-m <sup>2</sup>	223.325 kg-m <sup>2</sup>
Maximum angular rate	2.09 rad/s	1.050 rad/s
Limit	360°	-15° ~ 85°

Figure 2 indicates the layout of the marine-used 20 mm twin machine gun. The gunner, who sits in between two barrels and wears a helmet with an aiming device, automatically directs the gun's elevation and traversing motions with no hand wheels. When the target appears, the gunner follows the target and determines its current position in bearing and elevation along the line of sight (LoS) using the aiming device. Let the angular deviations between the barrels and LoS be  $\phi$  and  $\theta$ , the control loop always automatically drives a tracking loop to keep the barrels pointing at the target. This simplified control loop can continuously attack a target if the gunner follows the specific target.

The stabilisation of weapons and sensors in a ship is always an essential design consideration. The gun mount is fixed on the ship's deck. When the gun elevates and traverses in a plane perpendicular to the horizontal plane, the stabilisation must compensate for this tilt. As required, the gun carriage drive motors must continuously maintain the gun bore axis in the original direction. The tracking loop includes the stabilisation loop that keeps gun carriages rotating related to a reference. The stabilisation loop,

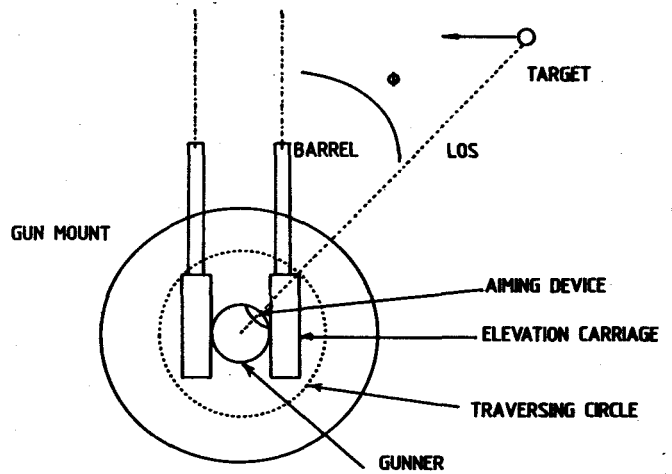


Figure 2(a). Top view of 20 mm twin machine gun

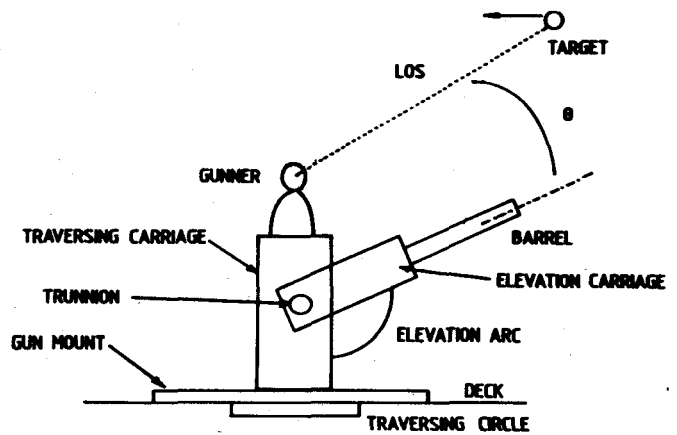


Figure 2(b). Side view of 20 mm twin machine gun

referred to as the inner loop, yields faster responses than the tracking loop, i.e., outer loop that makes tracking and firing at a stabilised platform for accurate requirement. Consequently, the stabilisation loop has a rate feedback. Figure 3 presents the simplified control loop for both bearing and elevation of the marine-used 20 mm twin machine gun.

### 3. HUMAN EFFECTS

The fire control for 20 mm twin machine gun in Fig. 3 is a typical man-in-loop and is deeply influenced by gunner's behaviour which also depends on aiming device, training, battlefield situations, and fight. The modelling of human behaviour remains a significant issue for sociology

\* See Appendix 1

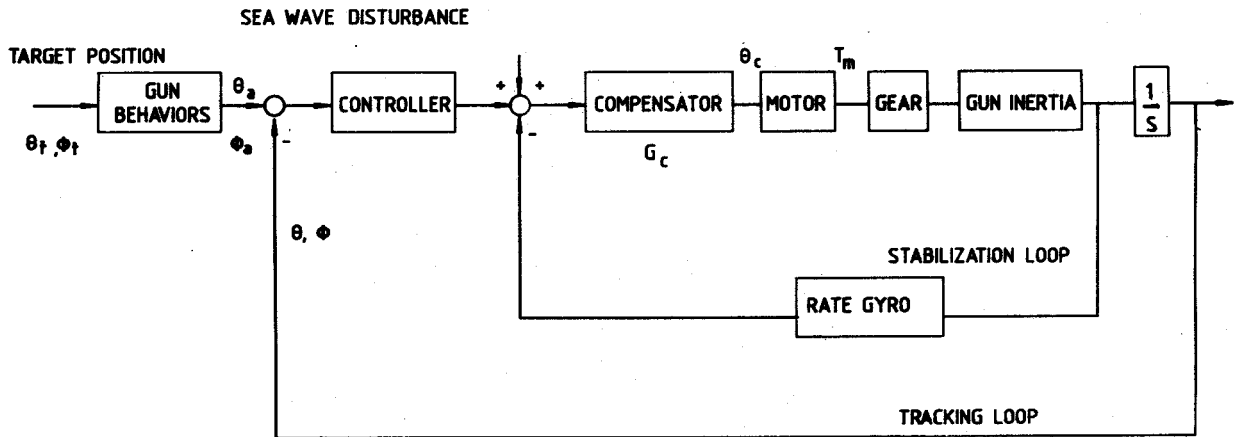


Figure 3. Control loop for 20 mm machine gun

and engineering. A rough model was made in control engineering<sup>6</sup>. Its gain stability in frequency response keeps well with small phase lag around  $0.15 \leq \omega \leq 1\text{Hz}$  that encourages this work.

The major concern in tracking loop design is the effects of the gunner's behaviour. No matter what kind of behaviour model is there, its final effect to the fire control performances is the time lag which may induce instability and tracking error problems. Therefore, the gunner behaviour's transfer function was allowed to be

$$\frac{\theta_a(s)}{\theta_t(s)} = \frac{\phi_a(s)}{\phi_t(s)} = e^{-\tau s} \quad (1)$$

where  $\tau$  denotes time delay caused by the gunner. The values of  $\tau$  may be different for different countries. The empirical values of  $\tau$  for a typical Chinese<sup>7</sup> are:

$$\begin{aligned} \tau &= 0.1\sigma && \text{for well-trained} \\ \tau &= 0.2\sigma && \text{in general} \\ \tau &= 0.4\sigma && \text{for poor-trained gunner} \end{aligned} \quad (2)$$

In this design, the worst case is taken to allow  $\tau = 0.4 \text{ s}$ .

#### 4. MATHEMATICAL MODELS

Once the control loop is established, the mathematical models for each block are derived.

#### 4.1 Angular Motion of the Gun

Since T75 gun mount is fixed on the deck, there is no translational motion but only rotational motion. According to the gun motion's dynamics, the gun's torque<sup>8</sup> can be expressed as

$$\sum T = \frac{dH}{dt} \Big|_s = \frac{dH}{dt} \Big|_g + \omega \times I \cdot \omega \quad (3)$$

In Eqn (3),  $H$  denotes its angular momentum,  $\omega$  angular velocity, and  $I$  moment of inertia of the gun. Subscripts  $s$  and  $g$  imply ship and gun, respectively. By defining the coincidence of the centre of gravity with the gun mount and the gun, the angular motions of the gun can be modelled as

$$T_t = I_t \ddot{\phi} \quad \text{bearing} \quad (4)$$

$$T_e = I_e \ddot{\theta} \quad \text{elevation} \quad (5)$$

where

$T_t, T_e$  : Torque of gun mount in bearing and elevation, respectively

$I_t, I_e$  : Moments of inertia in bearing and elevation, respectively

$\ddot{\phi}, \ddot{\theta}$  : Angular accelerations in bearing and elevation, respectively.

Dampers are added on each axis to effectively suppress the gun's oscillation and to satisfy design specifications, where  $B$  denotes damping ratio

(Fig. 4). Therefore, the gun rotations' transfer functions are:

$$\frac{s\phi(s)}{T_i(s)} = \frac{1}{I_i s + B_i} \quad \text{bearing} \quad (6)$$

$$\frac{s\theta(s)}{T_e(s)} = \frac{1}{I_e s + B_e} \quad \text{elevation} \quad (7)$$

According to motor constant stall torque (9.04 N-m) and angular rate of elevation or bearing ( $120^\circ \text{ s}^{-1}$  or  $60^\circ \text{ s}^{-1}$ ), and using the final-value theorem, damping ratios in bearing and elevation,  $B_i = 8.636$  and  $B_e = 4.318$ , can be determined.

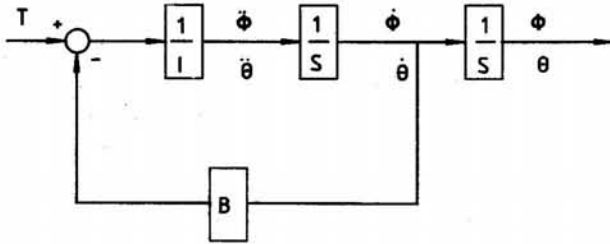


Figure 4. Block diagram for gun traversing and elevating motion.

#### 4.2 Motor & Gear Box

Two motors can drive 20 mm twin machine gun for elevation and bearing through gear boxes on two axes independently. DXM-480 motor of the Emerson Co. is used in the design. The transfer function of the motor is modelled as

$$\frac{T_m(s)}{s\theta_c(s)} = \frac{k_m}{\tau_m s + 1} \quad (8)$$

where

$$k_m = \frac{T_s N_s}{E(T_s + N_s f_m)}$$

and

$$\tau_m = \frac{I_m N_s}{T_s + N_s f_m}$$

$T_s$ ,  $N_s$ ,  $E$ ,  $f_m$ , and  $I_m$  are constant stall torque (9.04 N-m), maximum rotation speed (3000 rpm), operation voltage (115 V), friction coefficient (0.01), and rotor moment of inertia<sup>9</sup> ( $8.72 \times 10^{-4} \text{ kg-m}$ ),

respectively. Substituting these values into Eqn (8), one gets

$$\frac{T_m(s)}{s\theta_c(s)} = \frac{90}{s + 45} \quad (9)$$

The gear box between the motor and the gun inertia does amplify motor's torque and transfer to the gun which directs pointing of barrels in a short time. From design requirements, 0.02 s rise time means that the motor requires to reach maximum rotation speed of 3000 rpm or reach static within 0.02 s. Motor rotates 309.75 rad within the settling time in that tracking loop, say 1 s. Therefore, the amplification of motor torque which is equivalent to the gear ratio  $\eta$  satisfies

$$\eta = \frac{309.75}{\omega_p} \quad (10)$$

where  $\omega_p$  denotes the maximum angular rate in bearing or elevation, say 2.09 rad/s or 1.05 rad/s, respectively. Considering deceleration efficiencies of gear box in practical use, those values are chosen (0.36) in both axes. Thus, set  $\eta = 108$  in bearing and  $\eta = 54$  in elevation.

#### 4.3 Rate Gyro

A rate gyro measures bearing or elevation angular speed in stabilisation loop to keep the pointing of barrel. Its transfer function can be approximated by

$$G_{gyro}(s) = \frac{1}{\left(\frac{s}{\omega_n}\right)^2 + \frac{2\zeta}{\omega_n} s + 1} \quad (11)$$

where  $\omega_n$  and  $\zeta$  are the natural frequency and damping ratio of the rate gyro, respectively. Choosing these characteristics,  $\omega_n = 94.25 \text{ rad/s}$  and  $\zeta = 0.78$  are taken for general consideration.

#### 4.4 Compensator

For matching true motion of the gun, inserting compensator in bearing and using pole-zero

cancellation design technique, the transfer function of compensator is:

$$G_c(s) = \frac{0.85 (s^2 + 45s + 0.324)}{s^2 + 2.926s + 4.3681} \quad (12)$$

After this compensation, the dynamics of the gun will meet the open loop characteristics, which is 2.09 rad/s and 1.05 rad/s for bearing and elevation, respectively.

**5. CONTROLLER DESIGN**

Controller design is an essential parameter for achieving required stability and design specifications. In fire control design, putting PID and PI controllers in inner and outer loops to reduce cost and complexity, is a more realistic and convenient compensation. The forms of PID and PI controllers<sup>10</sup> are:

$$G_{PID}(s) = \frac{K_D s^2 + K_p s + K_I}{s} \quad (13)$$

$$G_{PI}(s) = \frac{K_p s + K_I}{s} \quad (14)$$

where  $K_D$ ,  $K_p$  and  $K_I$  denote tunable constants for derivation, proportion, and integration, respectively. In regular procedures, these constants must be

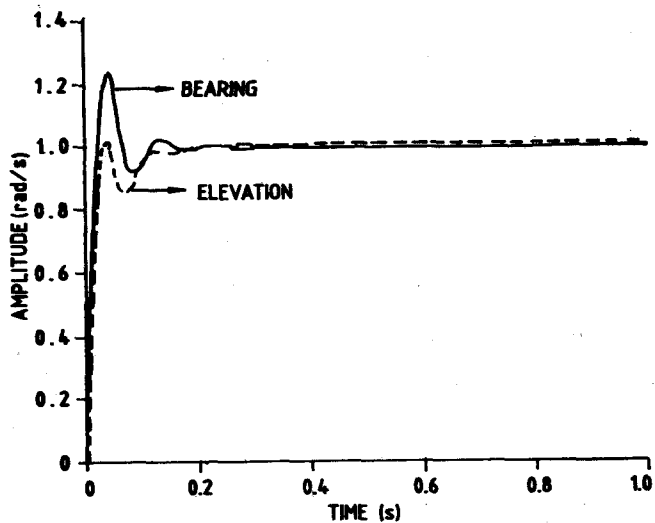


Figure 5. Step response for stabilisation loop

Table 2. Relative stabilities for the designed control loop

	Bearing		Elevation	
	Stabilisation	Tracking	Stabilisation	Tracking
Rise time (s)	0.020	0.319	0.022	0.303
Settling time (s)	0.101	0.410	0.099	0.326
Steady-state error (%)	0	0	0	0
Gain margin (dB)	2.875	24.220	3.441	Large enough
Phase margin (deg)	47.500	87.310	68.650	82.730

tuned on the basis of the time responses to satisfy required performances.

After some processes, these controllers can be obtained. These are:

$$G_{PID}(s) = \frac{7s^2 + 20s + 32}{s} \quad \text{bearing} \quad (15)$$

$$G_{PID}(s) = \frac{1.3s^2 + 30s + 5}{s} \quad \text{elevation} \quad (16)$$

$$G_{PI}(s) = \frac{7s + 0.1}{s} \quad \text{both bearing and elevation} \quad (17)$$

Figures 5, 6, and Table 2 demonstrate the step responses and relative stability of a complete system.

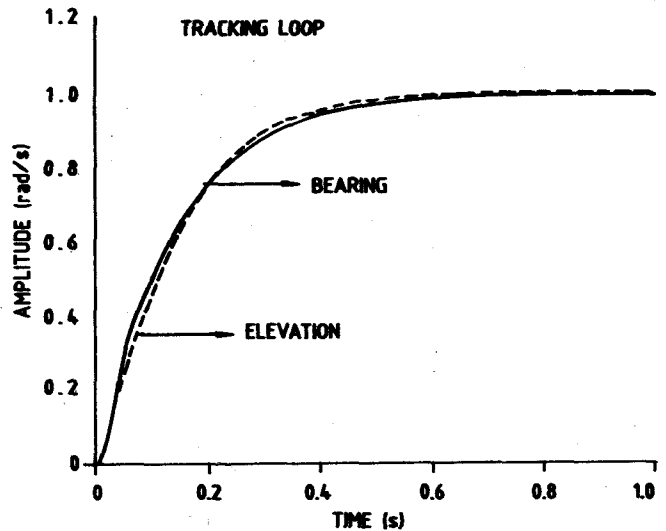


Figure 6. Step response for tracking loop

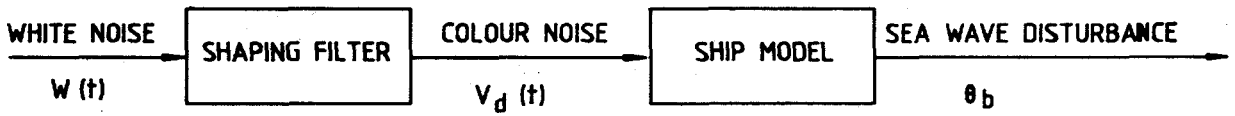


Figure 7. Generation of sea wave disturbance

6. NUMERICAL SIMULATIONS

6.1 Sea Wave Disturbance Model

When the sea wave swells the ship, construction of disturbance model is the first parameter to provide an analysis baseline. Sea waves natural motion can be modelled as colour noises in simulation. Figure 7 presents the generation of sea wave disturbance.

The differential equation of shaping filter<sup>4</sup> is:

$$\dot{V}_d(t) = -\beta V_d(t) + \sqrt{2\beta\sigma^2} W(t) \tag{18}$$

where  $\beta$  and  $\sigma^2$  denote the inverse of correlation time and required variance of  $V_d$ .

As the sea wave strikes the ship's body, it subsequently transmits a colour force to the gun mount which yields a tilt angle to the ship and gun. The ship model describes the relationship between colour noise and tilt angle of gun mount and carriage. It can be modelled as a second-order form<sup>4</sup>

$$J_h \ddot{\theta}_b(t) + D_{se} \dot{\theta}_b(t) + K_{se} \theta_b(t) = V_d(t) \tag{19}$$

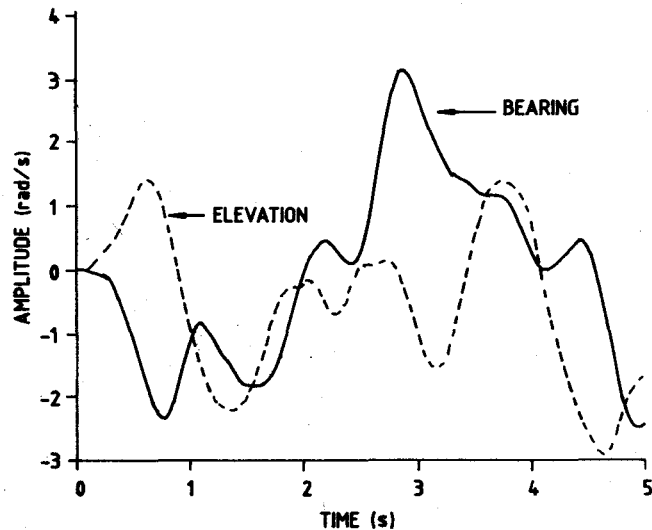


Figure 8. Sea wave disturbances input

where  $\theta_b$  expresses the tilt angle of ship,  $J_h$ ,  $D_{se}$ , and  $K_{se}$  represent moment of inertia, swelling damping ratio, and spring constant of ship, respectively. For a certain ship,  $J_h = 17300$  kg-m-s<sup>2</sup>,  $D_{se} = 12110$  kg-m-s, and  $K_{se} = 986100$  kg-m-/rad. Therefore, the transfer function of disturbance generation can be expressed as

$$\frac{S\theta_b(s)}{W(s)} = \frac{\sqrt{2\beta\sigma^2}}{s+\beta} \cdot \frac{0.000058s}{s^2 + 4.5s + 57} \tag{20}$$

6.2 Stabilisation Analysis

The study demonstrates stabilisation performances with disturbance inputs only and without time lag induced by the gunner's operations. A standard normal distributed  $W(t)$  is utilised to generate a colour noise,  $V_d$  in Eqn (18). The generation of sea wave disturbance results in disturbance inputs with maximum amplitude up to 3 rad/s (171.9°/s) in bearing and -3 rad/s (-171.9°/s) in elevation that cause rather large tilt angles in a ship (Fig. 8). For gun carriages, Fig. 9 indicates the responses in angle displacement whose maximum angles are only 0.037 rad (2.22°) and -0.03 rad (-1.719°) in bearing and elevation,

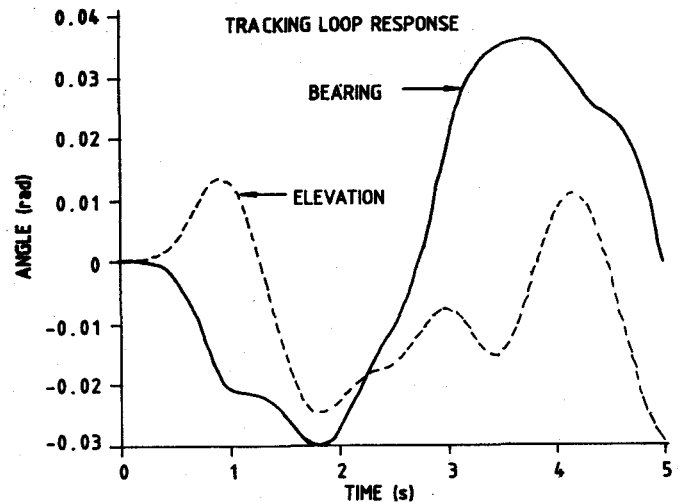


Figure 9. Angle responses under sea wave disturbances input

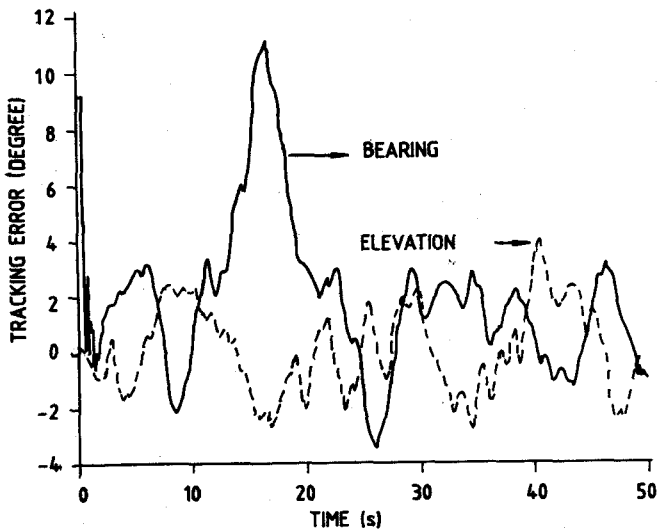


Figure 10. Tracking error in Scenario 1

respectively. These results have demonstrated that the T75 gun's stabilisation ceases a large disturbance from a sea swelling that provides a basis for an accurate pointing.

### 6.3 Accuracy Analysis

The main objective of T75 gun development was to provide defence against air threat, particularly in low-flying attack, e.g., antiship missiles and pop-up targets. Two scenarios called cross-over and pop-up Scenarios are presented here. The gunner in the loop causes time delay of 0.4 s.

#### 6.3.1 Scenario 1: Cross-Over

Scenario 1 simulates the engagement of a target crossing over a ship with constant speed  $v = 300$  m/s, altitude  $z = 20$  m, and off-range  $y = \pm 800$  m. The sea wave disturbances are shown in Fig. 8. After the stabilisation and tracking loops, the tracking error is shown in Fig. 10. In bearing axis, the maximum error up to  $11^\circ$  which occurs just in  $\phi = 90^\circ$ , and the other errors within  $13 \leq t \leq 19$  s are bounded in  $\pm 3^\circ$ . The tracking errors in elevation are also bounded in  $\pm 3^\circ$  except for near at  $t = 41$  s when target slips away from the ship.

#### 6.3.2 Scenario 2: Pop-Up

The pop-up flight path presents the typical attack from an aircraft to prevent detection by radar in a ship and the antiship missile with a sudden

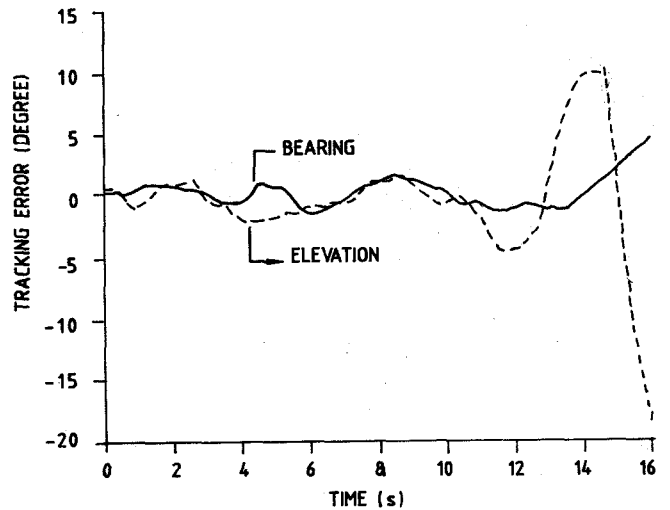


Figure 11. Tracking error in Scenario 2

appearance. Target position and speed are the same as in Scenario 1, but  $y = 10$  m. Target climbs up to 400 m within a range of 1200 m to the ship and then plunges down to attack. Figure 11 demonstrates the tracking errors in bearing and elevation which become large when the target flies up at  $t = 12.5$  s and dives at  $t = 14.5$  s. The maximum error in the other time is up to  $-5^\circ$  around  $t = 12$  s and the other errors are all bounded within  $\pm 2^\circ$ . A pop-up target's interception must obviously give an accurate pointing before taking a dive. These errors should be refined and covered by adjusting gun directions in achieving accuracy.

## 7. CONCLUSIONS

This paper presents a tracking loop's preliminary design for shipboard T75 twin machine gun to strengthen point defence ability on a battleship used. It uses a direct type fire control to follow and engage targets. Compensator and controllers are designed for achieving these requirements. Simulation results indicate that stabilisation of gun mount and carriage under a rather large sea wave disturbance is a good design. It also demonstrates the tracking capability by two scenarios simulation that the tracking errors can converge in a bounded region. The above errors should be covered by adjusting gun directions in future designs. The man-in-loop tracking system

yields simple and low cost advantages. Gunner's behaviour is undoubtedly the dominant factor and should provide effective training to reduce the man-made errors.

## REFERENCES

1. Crose, C.D. (Jr). Introduction to shipboard weapons. Naval Institute Press, Maryland, 1975.
2. Binroth, W. Closed-loop optimisation program for the M60A1 tank stabilisation system, 1975. Report No. R-CR-75-011.
3. Neau, J. & Liu, J.J. Mathematical model establishment and performance analysis of stabilisation system of a tank. *J. Chung Cheng Inst. Technol.*, 1992, 20(2), 113-21.
4. Wu, C.F. Stabilisation loop design for the shipboard 20 mm twin machine gun. Chung Cheng Institute of Technology, Republic of China, 1996. Master Thesis.
5. Servo system of 20 mm twin machine gun. Ching Ling Industrial Centre. National Taiwan University, Taipei, 1994.
6. Moh, T.C. Stabilisation system of machine guns. *In* Short course on weapon system engineering, Department of System Engineering, Chung Cheng Institute of Technology, Tao Yuan, 1996. pp. D 20-D 23.
7. Chiang, C.M. Human engineering. Shu Publication Co., Taipei, 1995. p. 158.
8. Greenwood, D.T. Principles of dynamics. Prentice-Hall, New Jersey, 1988.
9. Emerson, Emc. Positioning drives and motors. Emerson Corp., 1989.
10. Ogata, K. Modern control system. Prentice-Hall, New Jersey, 1990.

## Contributors



**Dr Sou-Chen, Lee** received his MS and PhD in System Engineering both from the Chung Cheng Institute of Technology, Republic of China (ROC), in 1985 and 1993, respectively. He worked as Research Assistant at the Chung Shan Institute of Science and Technology, ROC during 1985-88. Since 1993, he has been working as Associate Professor in the Department of System Engineering, Chung Cheng Institute of Technology. His research areas include: inertial navigation system, guidance and control, and dynamic system.



**Mr Cheng-Yu, Liu** received his MS in System Engineering from the Chung Cheng Institute of Technology, ROC, in 1983. Since 1983, he has been working as Research Assistant at the Chung Shan Institute of Science and Technology, ROC. His research areas include: estimation, system identification and control theory. He is a student member of the Institute of Electronic, Information and Communication Engineers.

**Computation of Moment of Inertia**

For computing the moment of inertia involving the gun, the equivalent type has been shown in Fig. A-1. Thus, the moment of inertia wrt elevation axis is expressed as

$$I_e = \frac{1}{6} m(3r^2 + l^2) + \frac{1}{2} ml^2 + \frac{1}{2} M_2 R_2^2 \tag{A-1}$$

where  $m$  and  $M_2$  imply the masses of barrel and elevation carriage, respectively;  $r$  and  $R_2$  denote the equivalent diameters, and  $l$  the length of barrel. The moment of inertia ( $I_i$ ) composes the moments of inertia involving elevation carriage,  $I_{BZ}$  and training carriage,  $I_{AZ}$  wrt traversing axis.  $I_{AZ}$  can be expressed as

$$I_{AZ} = \frac{1}{2} M_1 R_1^2 \tag{A-2}$$

where  $M_1$  denotes the mass of traversing carriage and  $R_1$  represents the equivalent diameter of the traversing carriage.  $I_{BZ}$  is more complex that considers the moment of inertia involving the barrel and elevation carriage in  $X$  and  $Z$  axes.

Thus

$$I_{BZ} = 2(I_{BX}^2 \sin^2 \varphi + I_{BZ}^2 \cos^2 \varphi - 2I_{BXZ} \sin \varphi \cos \varphi) + \frac{1}{12} M_2 (3R_2^2 + 4d^2) + (M_2 + 2m)d_1^2 \tag{A-3}$$

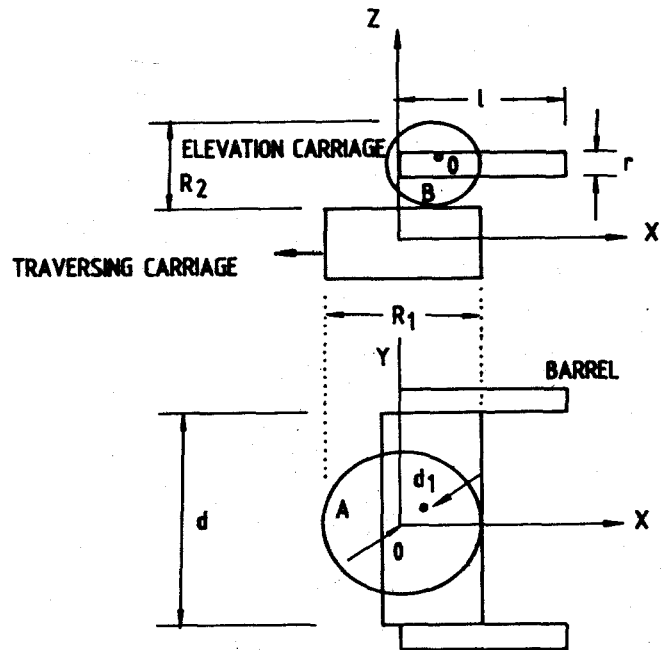


Figure A-1: Equivalent views for 20 mm machine gun

where  $I_{BX}$  and  $I_{BZ}$  represent the moment of inertia of  $B$  wrt  $X$  and  $Z$ ,  $I_{BXZ}$  denote the cross-moment of inertia.

Hence

$$I_i = I_{AZ} + I_{BZ} \tag{A-4}$$

By substituting real values into Eqn (A-1) ~ Eqn (A-4), the moment of inertia is obtained as shown in Table 1.